PROTEINS
STRUCTURE ■ FUNCTION ■ BIOINFORMATICS

Analyzing and modeling the inhibitory effect of phosphatidic acid on the GTP-γ-S binding activity of Goα

Liang Qu,[1] Jia Wan,[2] Yu Cao,[1] Yinghao Zhang,[1] Runsheng Chen,[2]* and Youguo Huang[1]*

[1] National Laboratory of Biomacromolecules, Institute of Biophysics, Chinese Academy of Sciences, Beijing 100101, People's Republic of China

[2] Laboratory of Bioinformatics, Institute of Biophysics, Chinese Academy of Sciences, Beijing 100101, People's Republic of China

ABSTRACT

G proteins are the molecular switches of G-protein-coupled signal transmembrane transduction, which plays a pivotal role in diverse cellular processes. The guanine nucleotide binding states of Gα-subunits are considered key factors for their functions. We report here that phosphatidic acid (PA) inhibits the [^{35}S]-GTPγS binding activity of Goα. To elucidate this inhibitory effect, biochemical analyses are carried out and a structure-based model is proposed. The experimental results show that PA particularly inhibits the activity of the Goα in a dose-dependent manner, whereas other lipids tested do not. Further analysis on the effects of PA analogs demonstrate that a phosphate head group together with at least one fatty acid chain is necessary for the inhibition. Using a lipid–protein binding assay, it is shown that Goα specifically and directly interacts with PA. In addition to these experimental studies, a 3D structure of Goα is constructed, based on sequence homology greater than 70% to E. coli Giα$_1$. Molecular docking is performed with PA and PA analogs, and the results are compared and analyzed. Collectively, the results of this investigation provide direct experimental evidence for an inhibitory effect of PA on GTP binding activity of Goα, and also suggest a structural model for the inhibitory mechanism. The lipid–protein model suggests that PA may occupy the channel for exchanging guanine nucleotides, thus leading to the inhibition. These findings reveal a potential new drug target for the diseases caused by genetic G-protein abnormalities.

Proteins 2008; 71:1732–1743.

***Key words:** phoshphatidic acid; lysophosphatidic acid; docking; modeling; Goα; modeling; G proteins; inhibition.*

INTRODUCTION

Heterotrimeric guanine-nucleotide-binding proteins (G proteins; subunits α, β, γ) play a pivotal role in signaling pathways by coupling the activation of heptahelical receptors at the cell surface to intracellular responses.[1–3] Numerous hormones, neurotransmitters or sensory stimuli exert their biological effects through these transmembrane receptors; and G-proteins in turn regulate the activity of various effectors such as enzymes and ion channels. In these processes, Gα-subunits act as molecular switches by transforming guanine nucleotide binding states.

Goα, a member of the Gi/Go family, is the most abundant Gα expressed in the brain.[4,5] Go proteins are activated by a common set of receptors[6] that include α2 adrenergic, D2 dopamine,[7] opioid, 5HT1, somatostatin, and the muscarinic M2 and M4 receptors. Goα-deficient mice display a severe impairment of motor control and a hyperalgesic response.[5] Several indirect evidences suggest that Goα functions independent of Gβγ. Constitutively active Goα promotes oncogenic transformation of NIH 3T3 cells,[8] and overexpression of Goα is sufficient to enhance neurite outgrowth in neuroblastoma cell lines including PC12[9] and Neuro2A cells.[10] It has also been proposed that some functions of Goα occur through the actions of free Gβγ dimers. Therefore, the timing and localization

Abbreviations: BODIPY, 4,4-difluoro-5,7-dimethyl-4 bora-3a,4a diaza-*s*-indacene-3-propionic acid; CH, cholesterol; DOG, 1,2-Dioctanoyl-*sn*-glycerol; DOPA, dioleoyl-PA; DPPA, dipalmitoyl-PA; GTPγS, Guanosine 5-3-*O*-(thio)triphosphate; HPA, 1-hexadecanoyl-*sn*-3-glycerol-phosphate; LPA, lysophosphatidic acid; LPC, lysophosphatidylcholine; PA, phosphatidic acid; PC, phosphatidyl choline; PE, phosphatidyl ethanolamine; PG, phosphatidyl glycerol; PI, phosphatidyl inositols; PS, phosphatidyl serine; SM, sphingomyelin; SUVs, small unilamellar vesicles.

Yu Cao's current address is Department of Physiology and Cellular Biophysics, Columbia University, New York, NY 10032.
Liang Qu and Jia Wan contributed equally in this work.
Grant sponsor: National Natural Science Foundation of China; Grant numbers: 30370350 and 30630040.
*Correspondence to: Runsheng Chen, Laboratory of Bioinformatics, Institute of Biophysics, Chinese Academy of Sciences, 15 Datun Road, Beijing 100101, People's Republic of China. E-mail: crs@sun5.ibp.ac.cn, or Youguo Huang, National Laboratory of Biomacromolecules, Institute of Biophysics, Chinese Academy of Sciences, Beijing 100101, People's Republic of China.
E-mail: huang@sun5.ibp.ac.cn
Received 9 March 2007; Revised 6 September 2007; Accepted 17 September 2007
Published online 3 January 2008 in Wiley InterScience (www.interscience.wiley.com).
DOI: 10.1002/prot.21826

of the guanine nucleotide binding states is a key to Goα signaling. Moreover, as a peripheral membrane protein, the structure and function of Goα may be influenced by the membrane environment surrounding it—in particular, the membrane lipid composition. Our observations suggested that phosphatidic acid (PA) might affect the [^{35}S]-GTPγS binding activity of Goα.

Over the last few years, the role of PA in cellular signal transduction has become a topic of great interest.[11–15] As a lipid second messenger, PA has been implicated in various cellular processes such as cell survival, cell proliferation, membrane trafficking, secretion, cytoskeletal rearrangement, and so forth. However, the direct interaction between PA and PA-binding proteins[16–18] has defied a clear description. It is believed that a specific structural fold, rather than a simple electrostatic interaction, is required for the PA–effector protein interaction. In addition, PA binding can directly modulate the activity of its effector enzymes (e.g. the GAP activity of RGS4, a regulator of G-protein signaling (RGS) protein, is inhibited by PA.[19]

In the present study, we report that PA specifically inhibits the [^{35}S]-GTPγS binding activity of Goα; and, based on the phenomenon observed, an interaction model of Goα and PA is proposed to explain the inhibitory mechanism.

METHODS

Guanosine 5-3-*O*-(thio)triphosphate (GTPγS) was purchased from Roche Molecular Biochemicals (Mannheim, Germany), and [^{35}S]-GTPγS was obtained from Perkin–Elmer (Boston, USA). PA, phosphadityl choline (PC), phosphatidyl serine (PS), phosphatidyl ethanolamine (PE), lysophosphatidylcholine (LPC), 1,2-Dioctanoyl-*sn*-glycerol (DOG), sphingomyelin (SM), and cholesterol (CH) were purchased from Sigma; and phosphatidyl glycerol (PG), phosphatidyl inositols (PI), cerebrosides, dioleoyl-PA (DOPA), and dipalmitoyl-PA (DPPA) were purchased from Avanti Polar Lipids (Alabaster, AL). 2-(4, 4-difluoro-5,7-dimethyl-4-bora-3a, 4a-diaza-*s*-indacene-3-pentanoyl)-1-hexadecanoyl-*sn*-glycerol-3-phosphate, diammonium salt (β-BODIPY FL C5-HPA) was from Invitrogen, product number D3805. All chemicals were of analytical grade. The expression plasmid pQE60-Goα was a gift from Prof. Susanne Mumby (University of Texas, Southwestern Medical Center), and the *N*-myristoyltransferase expression plasmid pBB131-NMT was a gift from Prof. Jeffrey Gordon (University of Washington). Anti-Goα rabbit polyclonal antibody and second goat antirabbit IgG-AP were obtained from Santa Cruz Biotechnology (Santa Cruz, CA).

Treatment of lipids

Aliquots of various phospholipids in chloroform stock solutions (stored at −20°C) were diluted with a 1-mL mixture of methanol/chloroform (1:3, V/V), and then dried under a stream of nitrogen gas. After storage under vacuum for 3–5 h to remove remaining organic solvent, the dried lipids were re-suspended in buffer A (see below) at 4°C by sonication with a probe tip sonicator (Ultrasonic Homogenizer, CPX 600) using 5 s-on/5 s-off pulses for altogether 10 min at 20% power. The resulting aqueous suspensions were pellucid or partly pellucid.

Expression and purification of myristoylated Goα

Myristoylated Goα was prepared by a method modified from Huang and coworkers.[20,21] *Escherichia coli* strain JM109 was co-transformed with plasmids pQE60-Goα and pBB131-NMT, and grown in T7-enriched medium (2% tryptone, 1% yeast extract, 0.5% NaCl, 0.2% glycerol and 50 m*M* KH_2PO_4, pH 7.2, supplemented with 50 μg/mL kanamycin and 50 μg/mL ampicillin). Isopropyl-β-D-thiogalactoside was added to a final concentration of 60 μ*M* when the OD_{600} reached 0.4–0.6, and the cells were then grown at 30°C overnight. The cells were harvested in buffer TEDP (50 mmol/L Tris, pH 8.0, 1 mmol/L EDTA, 1 mmol/L DTT, 0.1 mmol/L PMS), lysed by freezing-thawing with liquid nitrogen, and digested with lysozyme at 0.2 mg/mL. The lysate was centrifuged at 30,000*g* for 1 h. The supernatant was applied to a DEAE Sephacel column and eluted with 300 m*M* NaCl. The DEAE elute was adjusted to 1.2*M* $(NH_4)_2SO_4$ and 25 μ*M* GDP, and then applied to Phenyl Sepharose and Q Sepharose columns for further purification. Purity of Goα was evaluated by SDS-PAGE stained with Coomassie blue R-250, and the protein concentration was determined using the BCA™ Protein Assay Kit (Pierce). Generally over 70% purified Goα presented corresponding GTPγS binding activity.

[^{35}S]-GTPγS binding activity

The [^{35}S]-GTPγS binding assay was performed according to a slightly modified Northup *et al.*'s method.[22] Purified Goα was diluted to ∼800–1200 n*M* (for the assay of the GTPγS binding activity) with buffer A (50 m*M* Hepes, pH 8.0, 1 m*M* EDTA). Duplicate reactions were pre-incubated in the presence or absence of the lipid for 30 min at room temperature. The reactions were then initiated by the addition of 5 μ*M* ^{35}S-labeled substrate GTPγS and 20 μL buffer B (50 m*M* Hepes, pH 8.0, 1 m*M* EDTA, 20 m*M* $MgCl_2$, 0.05% Lubrol PX), allowed to proceed for 45 min at 22°C, and then stopped with the addition of 1.5 mL cold buffer C (20 m*M* Tris, 100 m*M* NaCl, 25 m*M* $MgCl_2$). The samples were then passed through 0.22 μm cellulose nitrate films, after which the films were sufficiently washed with 12 mL buffer C and dried at room temperature. Scintillation counts were performed in a liquid scintillation counter

(Model 1450, Perkin–Elmer) with the addition of 2 mL scintillation liquid.

Goα lipid-binding assays

Purified Goα was diluted in buffer D (20 m*M* Hepes, pH 8.0, 1 m*M* EDTA) with the addition of excess GDP. Different concentrations of the various phospholipids were also prepared in buffer D. Binding reactions were carried out in 45 μL buffer D, and then incubated for 30 min at 22°C. The samples were adjusted to a final concentration (20 m*M* Hepes, pH 8.0, 1 m*M* EDTA, 2 m*M* $MgCl_2$, 100 m*M* NaCl) by adding 5 μL buffer E (20 m*M* Hepes, pH 8.0, 1 m*M* EDTA, 20 m*M* $MgCl_2$, 1000 m*M* NaCl). The resulting samples were pelleted at 18,000 rpm at 4°C for 30 min (Micro 22R Zentrifugen). The phospholipid-Goα containing pellets were rinsed twice with buffer D plus 2 m*M* $MgCl_2$ and 100 m*M* NaCl. Then the pellets were re-suspended in the sample buffer for SDS-PAGE analysis. Goα bound to various phospholipids were analyzed by SDS-PAGE or Western blotting.

Fluorescence resonance energy transfer method

Fluorescence resonance energy transfer (FRET)[23,24] between tryptophan residues in the Goα protein (excitation at 280 nm) and β-BODIPY in the phospholipid (emission at 515 nm) was used to monitor the association of protein with PA.[25] Direct excitation of the BODIPY group at 280 nm produced a reference emission intensity (F_0). Fluorescence energy transfer was expressed as $(F - F_0)/F_0$, where F and F_0 are the fluorescence emission intensities of phospholipid at 515 nm with and without addition of Goα, respectively. β-BODIPY FL C_5-HPA was mixed at 5 mol% in SUVs with the desired phospholipid compositions. The measurements were performed at 25°C in a Hitachi F4500 fluorescence spectrophotometer.

Homology modeling and molecular docking

All of the molecular mechanical calculations were done with the aid of the software package InsightII (MSI, http://www.accelrys.com/products/insight/) on an SGI graphic workstation (Silicon Graphics, USA) under CVFF (consistent valence force field).

Modeling and refinement of the 3D structure of Goα

To find homologous proteins of Goα with known 3D structures, a sequence search using the NCBI online server Blastp was performed (database: PDB, http://www.ncbi.nlm.nih.gov/blast/Blast.cgi). Seven structures of *E. coli* $Gi\alpha_1$ returned the highest scores: Score = 512 bits, E value = 4 E−146, Identities = 255/354(72%), Positives = 293/354(82%), Gaps = 2/354 (0%). The two gaps found in these were a Lys101 insertion and a Lys312 deletion. The sequences with the most integrated structure (PDB id: 1AGR, A chain)[26] and the highest resolution (PDB id: 1GDD, resolution: 2.2 Å, missing 202–217 and 234–239 coordinates)[27] were selected among the seven $Gi\alpha_1$ structures. These two sequences were then joined together[28] to a whole template for modeling the 3D structure of Goα using the homology module of InsightII. Residues 1–5 were not modeled because none of the seven proteins provided coordinates in this region; in addition, this N-terminal region is located far from the guanine nucleotide binding domain. After adding hydrogen atoms and capping the N- and C-terminal residues, a crude model for residues 6–354 was obtained. The crude model was refined by the energy minimization program in the Discover3 module to 0.5 kcal/(mol*Å). The final structure was then superimposed on the backbone of the former structure (before refinement), and evaluated with the aid of Profiles-3D/Verify in the Homology module. Profiles-3D provides tools to measure the compatibility of an amino acid sequence with a three-dimensional structure by reducing the structure to a one-dimensional representation.[29,30] And the program Profiles-3D/Verify can be used to assess the validity of hypothetical protein structures by measuring the compatibility of the hypothetical structure with its own amino acid sequence. If the self-compatibility score given by Verify is close to the value expected for a correct structure of a same length sequence, then the structure is relatively reliable.

GTP docking with Goα

Consulting the GDP position in homologous proteins (such as 1ARG), GTP was manually positioned into the active pocket of Goα. Residues within 6 Å around GTP were defined as the binding region, and allowed to vary during the docking process whereas all other residues were kept fixed. Subsequently, simulated annealing docking[31] was applied with the aid of the Docking module according to the following four steps:

1. The system was defined in the Affinity/Setup_System (parameter confine ligand was set to 3 Å).
2. All of the flexible dihedral angles in GTP were defined, the maximal torsion angle change allowed being 180°.
3. One hundred random samplings were carried out,[32] screening for the best 20 structures.
4. Simulated annealing was performed on the 20 structures by cooling the whole system slowly from 480 to 280K, then minimizing the structural energy in 1000 steps using the conjugate gradient algorithm.

All frames were analyzed according to the same three principles: whole system energy, intermolecular energy, and Ludi score. Ludi program is useful for de novo

design of ligands for proteins, management of candidate ligand fragments and scoring ligand–inhibitor complexes. A higher Ludi score represents a stronger binding of a ligand to the receptor. The Ludi score is correlated with the dissociation constant K_i (M)[33,34]: Score $= -100 \log K_i$.

PA docking with Goα

Executing a random sampling algorithm for PA docking is not possible because of its two long fatty acid tails and more than 30 dihedral angles. In addition, the binding region is unknown. Grid docking before simulated annealing was therefore performed as given in the following seven steps:

1. The Builder module was used to build the original conformation of PA, which has two parallel fatty acid side chains. Geometry was then optimized by 1000-step minimization.
2. The experimental results suggested that PA can inhibit the GTP binding activity of Goα; therefore, a possible PA-binding region was defined including the GTP binding pocket and the surface within 15 Å of the GTP purine moiety. The purpose of choosing such an extensive area was to find the most likely PA-binding site.
3. The starting structures were random conformations in which the phosphoric acid head of PA extends into the GTP binding site. Random sampling was done 10 times by the aid of the Docking module's Affinity/GridDocking, creating five structures each time.[35] Three dihedral angles in the PA head are flexible; the other angles, including the two side chains, are rigid. The grid resolution is 0.6 Å.
4. After eliminating distinctly undesirable conformations (such as PA binding far away from GTP binding pocket), there were 25 structures left. According to the tropism of PA, these complex structures were separated into three classes: parallel, antiparallel and upright (which include two contrary directions) in relation to the suppositional line connecting Lys67 and Lys280.
5. The two optimal structures with the lowest intermolecular energy were chosen from each class. After shrinking the binding region to 6 Å around PA, the position of PA was adjusted manually to move the phospholipid closer to the binding site, all the while modulating its position to avoid overlaps with the atoms of Goα. Grid docking with the 10 structures was then repeated to create five conformations each time. Grid resolution was 0.5 Å.
6. After eliminating impossible conformations, there remained 17 possible structures. Simulated annealing docking was then performed with every structure, keeping parameters the same as for GTP docking.
7. To find the optimal complex conformation, the total energy of the system (intermolecular energy and Ludi scores) was calculated for each of the 17 structures.

LPA and PS docking with Goα

In general, phospholipids comprise a hydrophilic head, a glycerol backbone and two fatty acid tails. LPA and PS have similar structures to PA. The differences between PA and these two lipids are that LPA has a single fatty acid tail whereas PA has two, and PS has a larger hydrophilic head than PA. The conformation of PA was therefore modified from the optimal complex (obtained as above), to create structures of LPA (by deleting the PA *sn*-2 tail) and PS (by adding atoms to the PA head and optimizing the geometry of its larger head). Under the assumption that LPA and PS dock with Goα in a similar manner to PA (because of their aforementioned structural similarities), LPA and PS were positioned in the optimal docking position of PA, and then turned or moved slightly to create five different starting complex structures, followed by simulated annealing docking as above. Parameters and evaluation were the same as for the PA docking.

RESULTS

PA specifically inhibits the [^{35}S]-GTPγS binding activity of Goα

Initially, Goα was incubated with various phospholipids and the [^{35}S]-GTPγS binding assayed. In particular, PA inhibited the GTPγS binding activity of Goα, whereas other phospholipids with different polar heads such as PC, PE, PS, and PG or other lipids like SM, CH, and CH + SM did not [Fig. 1(A)]. Lubrol (0.05%) used in the reaction system had no effect on the activity assay (data not shown). When Goα was incubated with increasing concentrations of PA, a dose-dependent inhibition of GTPγS binding activity was observed with an IC_{50} of about 30 μ*M* [Fig. 1(B)]. However, different concentrations of PC or PS did not show the same dose-dependent response. A lipid analog which lacks the phosphate head group, DOG, also had no effect on Goα activity even at a concentration of 50 μ*M* (data not shown).

In addition, Goα was incubated with liposomes made of PA and PC (Molar ratio 1:1), and the [^{35}S]-GTPγS binding activity was then assayed. As shown in Figure 1(C), the [^{35}S]-GTPγS binding activity was slightly inhibited when the concentration of the liposomes increased, compared with the strong inhibition by pure PA. This result suggests that the vesicle structure is disadvantageous for the inhibitory effect of PA.

Effects of phospholipids with different fatty acid side chains

A phospholipid molecule is characterized by a polar head, the fatty acid side chains and the glycerol linker. Because PA is shown to clearly inhibit the GTPγS binding activity of the Goα and phospholipids with other polar heads did not show a similar effect [Fig. 1(A)], the

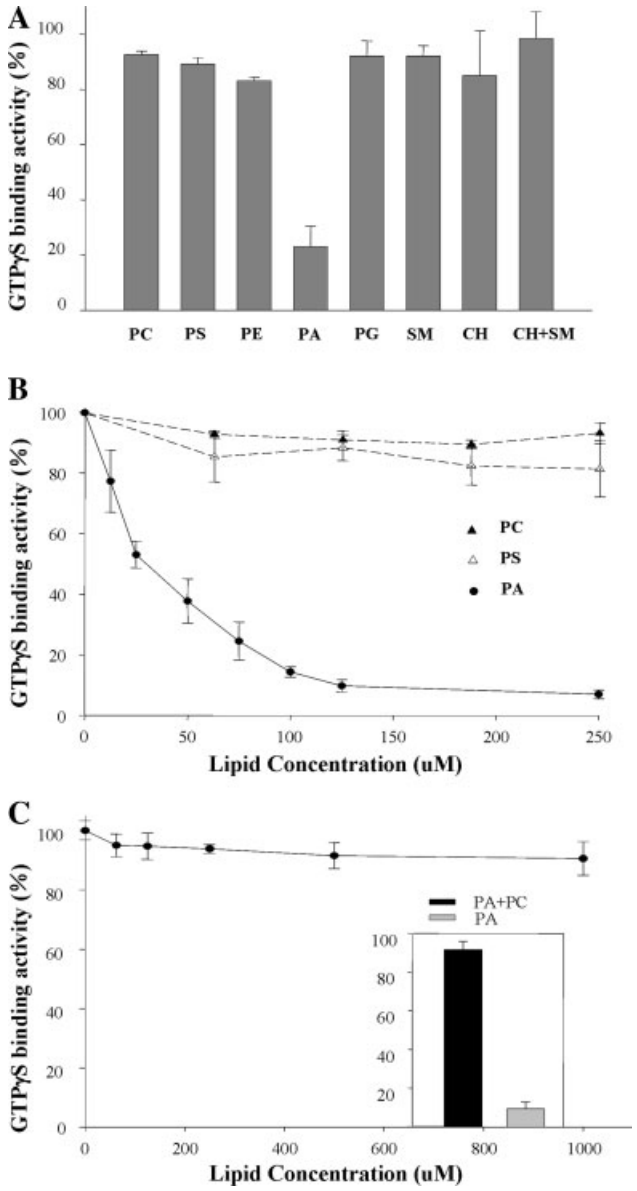

Figure 1

*Effect of various lipids on the [^{35}S]-GTPγS binding activity of Goα in vitro. (**A**) GTPγS binding activity was measured in the presence or absence of the different lipids, and the GTPγS binding activity in the presence of different lipids was expressed as percentage of the binding activity in their absence. SM and CH were mixed with PC in the molar ratio 1:2 for CH or SM alone, and in the molar ratio 1:1:1 for CH + SM, respectively. The final concentration of each phospholipid was 83 μM. (**B**) Effects of increasing concentrations of three lipids (PA, PS, PC) on GTPγS binding activity of Goα. These data represent the means ± SD of at least four experiments. (**C**) The GTPγS binding activity of Goα was measured in the presence or absence of liposomes composed of PA and PC (1:1 molar ratio) in which the total concentration of lipids was increased as indicated on the abscissa. The data represent the means ± S.D of at least three experiments. The small graph indicates the GTPγS binding activity of Goα measured in the presence of either 500 μM total lipids (PA:PC = 1:1) or 250 μM PA only.*

inhibitory effect of PA with different fatty acid side chains was evaluated. Figure 2 shows that DOPA and DPPA inhibited Goα binding activity to the same degree as PA [Fig. 2(A)], whereas LPA, which has only one fatty acid side chain, showed stronger inhibition of the binding activity of Goα with an IC_{50} of 7 μ*M*. LPC had no inhibitory effect [Fig. 2(B)]. With a final LPA concentration of 50 μ*M*, 100% inhibition of the GTPγS binding activity could be reached (data not shown).

Binding of Goα to PA/LPA

To distinguish whether the interaction between Goα and PA/LPA is direct or indirect, assays of the binding of Goα to various phospholipids were carried out (see Fig. 3). The results of both SDS-PAGE and Western blotting clearly indicated that Goα was able to bind directly to PA (3A.a&d) or LPA (3A.c&d). Moreover, the amount of bound Goα increased with increasing concentrations of PA/LPA (3A.d). Binding to other lipids such as PC, PE, PG (3A.a) PS, PI, CH, SM (3A.b), CH + SM, cerebrosides, and LPC (3A.c) were negligible. The SDS-PAGE mobility of the protein in the presence of PA was differ-

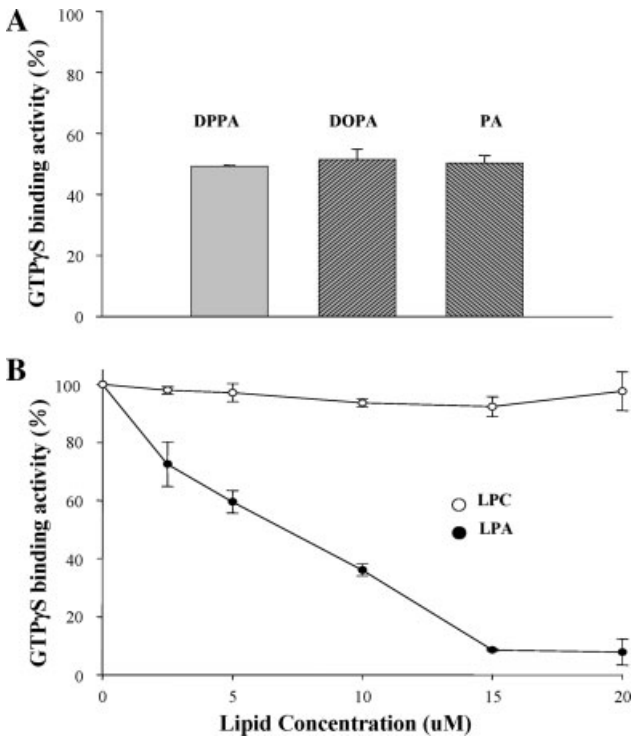

Figure 2

*Effects of PA variants with different fatty acid chains on the [^{35}S]-GTPγS binding activity of Goα. (**A**) The GTPγS binding activity of Goα in the presence of DOPA, DPPA, or PA was expressed as percentage of the control (in the absence of the lipids). The molar ratio of phospholipids to Goα was 50:1. The data are means ± SD of at least three replicate experiments. (**B**) Effects of increasing LPA or LPC concentration on the GTPγS binding activity of Goα (expressed as in Fig. 1). The data represent the means ± SD of at least three replicate experiments.*

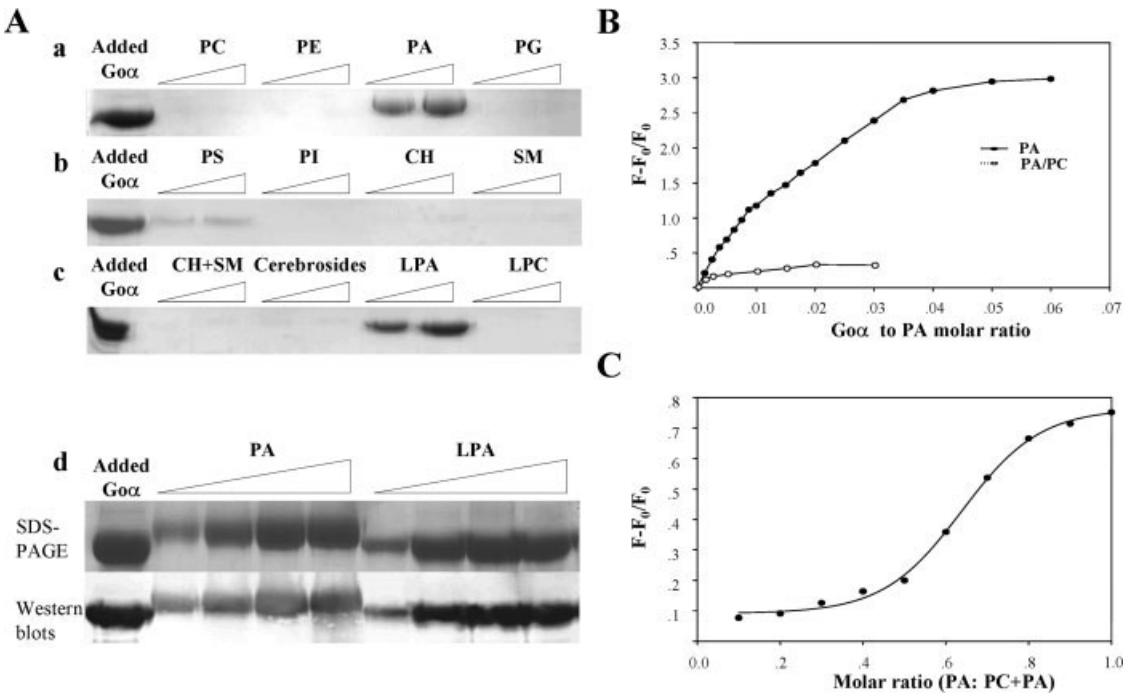

Figure 3

*Assays of lipids bound to Goα. (**A**) Goα was incubated with different concentrations of pure lipids or lipid mixtures as labeled. Bound Goα was analyzed with SDS-PAGE and Western blotting. The added Goα without any lipids was used as a control. Concentrations of lipids used for the binding assay were 500 or 1000 μM for PC, PA, PE, PG (a), PS, PI, SM (b) and cerebrosides (c); 1000 or 2000 μM for CH (b); and 200 or 400 μM for LPA and LPC (c). (**B**) Association of Goα with vesicles of PA/PC or PA determined by FRET. SUVs were prepared from PC/PA/β-BODIPY FL C_5-HPA (50:45:5) or PA/β-BODIPY FL C_5-HPA (95:5) mixtures. The concentrations of phospholipids were 25 μM, respectively. (**C**) Association of Goα with SUVs of PA/PC determined by FRET at increasing molar ratio of PA to (PA + PC). The total lipid concentration was 10 μM with 5 mol% of β-BODIPY FL C_5-HPA, and the Goα:phospholipid molar ratio was 0.2:100. Excitation and emission wavelengths in (B) and (C) were set at 280 nm and 515 nm, respectively.*

ent from that of the control sample or samples containing LPA. One of the reasons for this might be that PA interaction leads to changes in the electric charge of amino acid functional groups in Goα.

According to the method of Sanchez-Bautista *et al.*[23] and Corbalan-Garcia *et al.*[24] the binding of Goα to vesicles was rather low. Therefore, the more sensitive FRET assay was used to further monitor the association of Goα with PA under different conditions [Fig. 3(B)]. Goα contains two tryptophan residues at positions 132 and 212, which can serve as donors. β-BODIPY FL C_5-HPA, labeled at one fatty acid side chain of the phospholipid, accepts tryptophan-donated energy from the protein and undergoes a change in its fluorescence intensity as the protein binds to phospholipids. As shown in Figure 3(B), there were significant increases in fluorescence at 515 nm when PA was titrated with Goα, whereas only a slight increase was observed in the presence of vesicles composed of PA and PC (molar ratio 1:1). This result indicates that the binding of Goα to a vesicle interface is much weaker than binding to pure PA, despite the increasing concentration of Goα.

To confirm this result, the association of Goα with liposomes made of PA and PC at an increasing PA/(PC + PA) molar ratio was monitored by FRET [Fig. 3(C)]. The total phospholipid concentration was fixed at 10 μ*M* with 5 mol% of β-BODIPY FL C_5-HPA. As shown in Figure 3(C), when the molar ratio of PA increased, the binding of Goα to phospholipid was greatly enhanced. When the molar ratio was less than 0.5, the FRET signal increased only slightly; whereas with a PA/PC + PA molar ratio greater than 0.5, the FRET signal increased steeply. This result correlates with the former one that the binding of Goα to a vesicle interface is much weaker than binding to pure PA.

The modeled 3D structure of Goα

After homology modeling and refinement, the quality of the Goα 3D structure was evaluated with respect to stability and rationality. The refined model was superimposed onto the original structure, resulting in a backbone root mean square deviation (RMSD) of 1.6 Å between the two. This is a very small deviation for a protein of

Table I
Evaluation of the Results of 20 GTP–Goα Complex Structures

Frame	TotalE	Ludi	InterE	Elec	VDW
1	*−1561.5*	817	*−255.2*	−201.2	−54
2	*−1544.4*	938	−240.3	−185.8	−54.5
3	*−1528*	950	−215.4	−153.7	−61.7
4	*−1525*	*1029*	*−352.9*	−309.4	−43.4
5	*−1516*	918	*−250.2*	−202.6	−47.6
6	−1511	797	−234.6	−184.2	−50.4
7	−1506.9	*1020*	−209.3	−160.7	−48.6
8	−1501	*1172*	−229.1	−259.2	−39.9
9	−1494.6	*1097*	−150.4	−105.9	−44.5
10	−1488.8	723	−99.2	−41.9	−57.3
11	−1486	*960*	−106.5	−71.3	−35.2
12	−1480.8	749	−218.1	−164.5	−53.6
13	−1480.3	928	−136.8	−92.2	−44.6
14	−1472.9	855	−169.1	−112.9	−56.1
15	−1469	731	−140.2	−90	−50.2
16	−1468.9	833	*−280.8*	−225.9	−54.9
17	−1467.1	781	−135.8	−96.8	−38.9
18	−1459.4	926	*−273.7*	−222.9	−50.8
19	−1457.6	637	−215.4	−167.5	−47.9
20	−1456.2	823	−101	−52.1	−48.9

Energy unit is kcal/mol. TotalE, total system energy; Ludi, the score given by the Ludi module; interE, intermolecular energy between receptor and ligand (given by the docking/evaluate program), which is equal to the electrostatic energy (Elec) plus the VDW energy (VDW). The top five frames for each scoring method are italicized.

this size, and the difference is mainly found at the N- and C-terminals and in the orientation of the side chains. Evaluating the rationality of the model with module Profiles-3D gave a compatibility score of 148.5 (expected value for a natural protein of the same size is 159.5), suggesting that the final structure is reasonably credible.

The modeled GTP–Goα complex

After 100 times random sampling and subsequent simulated annealing docking of the best 20% of the structures, 20 candidate complex structures were created. Total energy, intermolecular energy, and Ludi scores for these 20 structures (Table I) were calculated. One particular structure (labeled frame 4) was ranked among the top 25% for all of the three main evaluation methods. The following structural analysis is based on this structure.

GTP binds to Goα in a similar way as GDP or GTPγS binds to Gi1[26,36] [Fig. 4(A,B)]; the nucleotide stays in the middle of the binding pocket, with the purine moiety in the bottom (near the β-sheets to the left in A) and the phosphoric acid group at the mouth of the pocket (B). The Goα distortion introduced by the docking is small, as the backbone RMSD before and after docking is only 1.8 Å. The distortion is mainly on the side of the phosphoric acid radical of GTP, as shown in Figure 4(A).

The intermolecular energy term corresponds to the binding energy between receptor and ligand (given by the docking/evaluate program), which is a summation of electrostatic and van der Waals (VDW) energy contributions. The electrostatic energy between GTP and Goα is −309.4 kcal/mol, which is 88% of the intermolecular energy. Six hydrogen bonds were detected in the GTP–Goα complex by the aid of the Measure/H Bond function. Their positions are shown in Figure 4(C).

The modeled PA–Goα complex

To obtain PA–Goα complex structures, simulated annealing docking to the 17 candidate structures (from

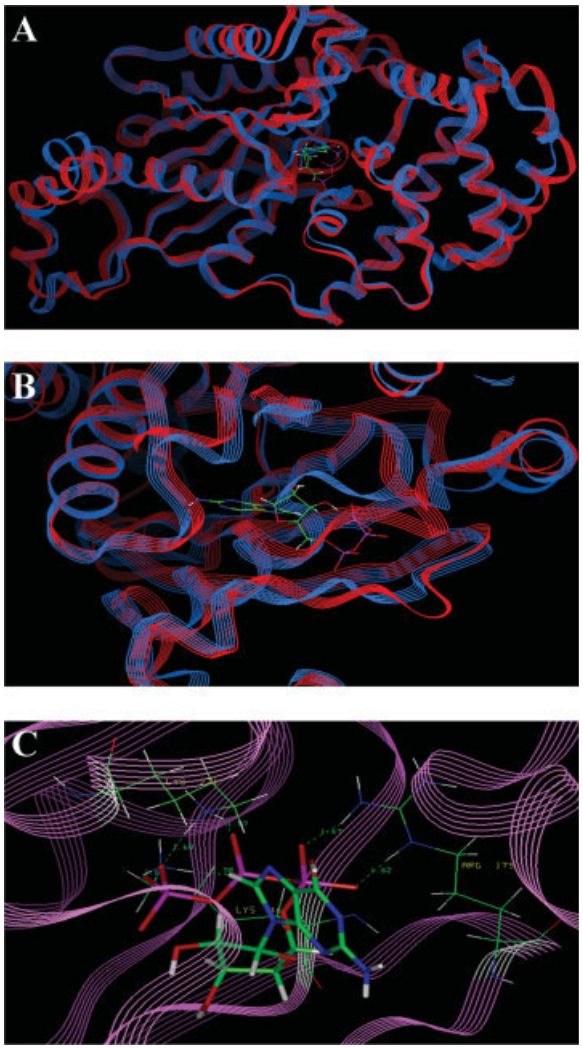

Figure 4
*Detailed view of the modeled GTP–Goα complex. Blue and red lines indicate the Goα ribbon before and after docking, respectively. (**A**) Structure of the entire complex with GTP shown in wire frame and Goα in backbone mode. (**B**) Same as in (A) except rotated 90°. (**C**) A more detailed view of the binding site. Goα is shown in backbone mode except for the three amino acids forming hydrogen bonds with GTP, which are displayed in wire frame. GTP is shown in stick mode. Six hydrogen bonds are shown as green broken lines with their lengths in Å. [Color figure can be viewed in the online issue, which is available at www.interscience.wiley.com.]*

Table II
Evaluation Results for the 17 PA–Goα Complex Structures

Class	Frame	TotalE	InterE	Elec	VDW	Ludi	H Bonds
I	1	−164.6	−150.8	−84.6	−66.2	160	*4*
	2	−253.6	*−176*	−93.7	−82.2	*393*	0
	3	−260.7	*−204.8*	−118.3	−86.4	*651*	*2*
	4	−126	−171.5	−102.4	−69.2	199	*3*
II	5	−263.4	−127.8	−59.7	−68.1	73	0
	6	−186.3	−132.7	−67.2	−65.5	78	1
	7	−262.3	−138.8	−61.3	−77.5	184	0
	8	−290	−124.1	−51.9	−72.2	−114	1
	9	*−358*	−117.9	−40.2	−77.7	125	1
III	10	−185.5	−141.8	−48.1	−93.8	96	1
	11	−145.7	*−171.6*	−90.8	−80.8	260	*3*
	12	−235.7	−152.9	−62.5	−90.4	*312*	1
	13	*−615.4*	*−217.5*	−139.6	−77.9	*502*	*3*
	14	−181.8	−155.9	−71.7	−84.2	248	1
	15	*−312.1*	−149.9	−80.4	−69.5	169	*2*
	16	*−406.7*	−153.1	−73.6	−79.5	197	1
	17	*−336.7*	*−183.4*	−84.6	−98.8	*522*	1

Explanations as in Table I.

grid docking) was performed, followed by structural classification. The results of the 17 simulations were then evaluated (Table II), indicating that frame 13 was the best candidate, with several characteristics different from the GTP–Goα docking model (see Fig. 5):

1. Two domains of the protein are spanned by PA. The two hydrophobic fatty acid moieties of the phospholipid (*sn*-1 and *sn*-2) cover the GTP-binding pocket (*sn*-2 is located outside, while *sn*-1 extends about 5 Å into the pocket. Deformation of the *sn*-1 tail gives it a distinct hook-like shape, which is clearly visible in Figure 5(A).
2. The backbone RMSD of Goα before and after docking is 0.81 Å. The distortion mainly occurs at a 324–335 aa fragment that includes a short loop and about two turns of an α-helix [shown in Fig. 5(A)]. This fragment comprises the binding site for the phosphoric acid head group and glycerol backbone. These observations suggest that the GTP binding pocket on the surface of Goα is enlarged by PA binding.
3. The electrostatic surface in the PA binding site is shown as solvent accessible surface in Figure 5(B). Electrostatic interactions between the ligand and receptor result in ∼64% of the total intermolecular energy. Hence, the VDW energy (about 36%), suggests that hydrophobic interactions [shown in Fig. 5(C)] are also important factors in the docking process.
4. Four potential hydrogen bonds between PA and Goα were identified. Considering that the hydrogen bond energy is much smaller than the energy difference between the various candidate structures, the number of hydrogen bonds is not considered to be a critical factor in determining the best complex structure.

The modeled LPA-Goα and PS-Goα complexes

For both LPA and PS, five candidate complex structures were created after simulated annealing docking, and then evaluated in the same way as for PA–Goα (Tables III and IV). The LPA–Goα complex [Fig. 6(A)] resembles the PA–Goα complex [Fig. 5(A)] but with a more extended

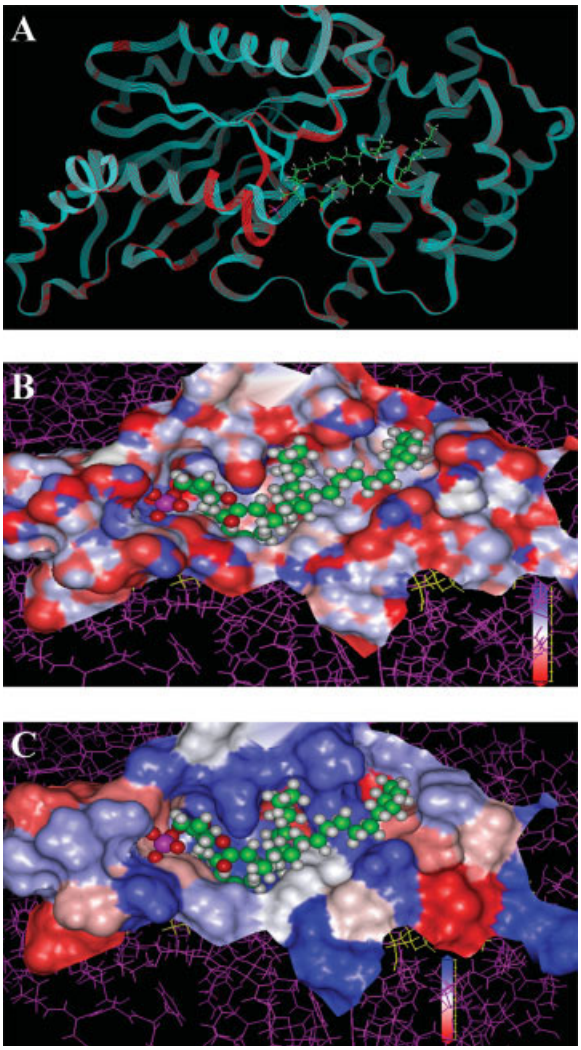

Figure 5
*Local structure of the modeled PA–Goα complex. (**A**) The PA–Goα complex. Goα is shown in backbone mode; green and red indicate Goα before and after docking, respectively. (**B**) Electrostatic surface. Goα is shown in wire frame, PA in space filling mode, and the binding site as solvent accessible surface. Red to blue shading indicates residues with increasing negative to positive charge shift. (**C**) Hydrophobic surface. Goα is shown in wire frame, PA in space filling mode, and the binding site as solvent accessible surface. Red to blue shading indicates residues with increasing hydrophobic shift.*

Table III
Evaluation Results for the Five LPA–Goα Complex Structures

Frame	TotalE	InterE	Elec	VDW	Ludi	H Bonds
1	−451.2	−187.1	−127	−60	473	2
2	−444.5	−183.2	−129.5	−53.7	474	3
3	*−479.3*	−182	−129.6	−52.3	249	2
4	−359.4	−182.8	−130.8	−52	393	3
5	−446.6	*−193.3*	−138.9	−54.5	*591*	*4*

Explanations as in Table I. The best frame for each scoring method is italicized.

LPA glycerol backbone. The PS–Goα structure [Fig. 6(B)] is also similar to that for PA–Goα; however, distortion of residues in the 324–335 fragment is more pronounced. As seen in the figure, the two turns of the α-helix unfold because of the huge head group of PS. Obviously, there would be a high-energy barrier between the apo- and PS-bound protein states. This observation indicates that the PS docking state of Goα is unlikely to occur, consistent with the experimental results.

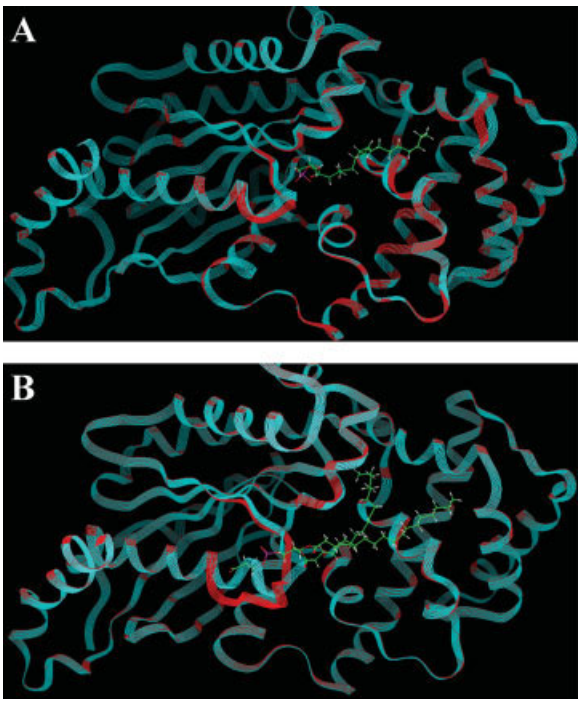

Figure 6
*Distortion of the Goα backbone by introduction of the two ligands LPA and PS. Goα is shown in backbone mode; green and red indicate Goα before and after docking, respectively. (**A**) LPA–Goα complex. (**B**) PS–Goα complex. [Color figure can be viewed in the online issue, which is available at www.interscience.wiley.com.]*

DISCUSSION

We have evaluated the specific effects of various membrane lipids on the GTPγS binding activity of the Goα subunit. The results clearly show that PA and LPA strongly and specifically inhibit the GTPγS binding activity of Goα [Figs. 1 and 2(B)]. PA is characterized by a phosphate head, two fatty acid side chains and a glycerol linker. The fact that anionic phospholipids such as PS and PG did not influence the activity of Goα suggests that a simple electric charge factor might not be sufficient to account for the inhibition. In addition, DOG, which is similar to PA apart from the phosphate head, had no effect on Goα activity even at a concentration of 50 μ*M* (data not shown). This observation suggests that the presence of the phosphate head is necessary for lipid binding. Further studies demonstrated that LPA, a derivative of PA with only one fatty acid chain, has a more potent inhibitory effect than PA [Fig. 2(B)]. Thus, a phosphate head group together with at least one fatty acid chain is necessary for the inhibition of Goα by the binding of PA or LPA.

Because PA and LPA are able to specifically inhibit the GTPγS binding activity of Goα, how does this inhibition happen? The direct interaction of Goα with PA was further evaluated using lipid–protein binding and FRET assays (see Fig. 3), which have proven to be the effective tools for probing lipid–protein interactions. Goα specifically binds to PA and LPA; however, it neither interacts with phospholipids like PC and PE, and so forth, nor with other lipids like SM and CH [Fig. 3(A)]. The binding results agree with the results from the [^{35}S]-GTPγS binding assays. To our knowledge, this is the first demonstration of a direct and highly specific interaction between Goα and PA or LPA. Moreover, the results from the FRET assay further indicate that the PA inhibition of the Goα binding activity may depend on free PA molecules, and that PA molecules as components of vesicles are less available for Goα binding [Fig. 3(B,C)].

To better understand the inhibitory effect of PA on Goα, homology modeling and molecular docking was employed to simulate the interaction between PA (or

Table IV
Evaluation Results for the Five PS–Goα Complex Structures

Frame	Total energy	Intermolecular energy	Electrostatic energy	VDW	Ludi	H Bonds
1	−461	*−187.7*	−101.6	−86.1	502	*5*
2	*−544.7*	−187	−88.6	−98.3	*639*	1
3	−490.5	−181	−101.3	−79.7	292	3
4	−500.4	−169	−101.9	−67.1	148	3
5	−509.2	−172.1	−82.8	−89.4	210	1

Explanations as in Table I. The best frame for each scoring method is italicized.

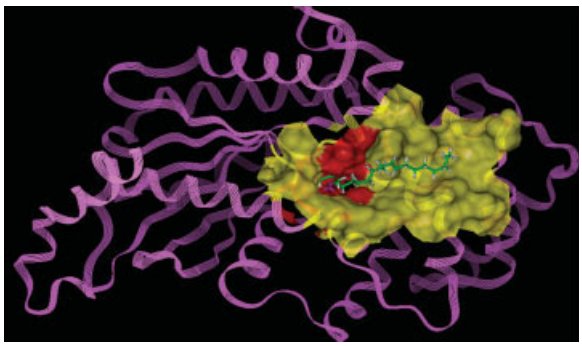

Figure 7

Relative positions of the LPA-binding site and the GTP binding pocket. The solvent accessible surface within 6 Å from LPA is displayed. Red color indicates amino acids within 2.5 Å from GTP in its binding pocket. Goα and LPA are shown in backbone and stick mode, respectively. For simplification, this figure only shows the interaction between LPA and Goα. The mode of interaction between PA and Goα is similar (not shown). [Color figure can be viewed in the online issue, which is available at www.interscience.wiley.com.]

LPA) and Goα. A model for the interaction between PA (or LPA) and Goα was constructed (Figs. 5 and 7), in which the phospholipid ligands span the GTP binding and α-helix domains of Goα, with their phosphate head groups pointing to the loop of the 326–331 aa residue fragment and with one fatty acid chain covering the guanine nucleotide binding cleft. The entire phospholipid molecule appears to cover over the guanine nucleotide-binding cleft, which is believed to be the channel for exchanging GTP for GDP. From this model, it can be reasonably speculated that PA (or LPA) occupies the structural channel in the enzyme wherein GTP–GDP exchange occurs. This, in turn leads to inhibition of the GTPγS binding activity of Goα (see Fig. 7).

When comparing the experimental results with the constructed model of interaction between PA (or LPA) and Goα, several clues become evident. First, the experimental data indicated that the phosphate head group together with at least one fatty acid chain is necessary and essential for the inhibition; the structure model showed that the interaction requires both VDW forces contributed by fatty acid chains and the electrostatic interactions provided by the phosphate head group, and, moreover, the model indicated that at least one fatty acid chain is needed to block the guanine-binding cleft. Second, the results of our experiments demonstrated that PA/LPA specifically inhibited the binding activity of Goα by direct interaction, whereas other phospholipids, for example PS, had no significant effect. The binding model for PA and Goα [Fig. 5(A)] can be shifted to PS [Fig. 6(B)], which at first glance may seem to form a rather stable interaction with Goα, however, the larger polar head of PS force a de-configuration of an α-helices (Table V), which would require a very high change in potential energy. We therefore speculate that the binding of Goα to PS would rarely happen. Third, the experimental study also assumes that LPA with only one fatty acid chain is a more potent inhibitor of Goα than PA. According to the model [Fig. 5(A)], besides the lower molecular weight and the less space occupied by LPA [Fig. 6(A)], the lesser structural change required involved in the interaction between Goα and LPA may explain the observed experimental results. The lipid–protein interaction model, which was set up by modeling and docking, indeed agreed well with the experimental results and offers an explanation for the mechanism behind the experimentally observed phenomena.

Two models for the mechanism behind G protein-coupled signal transduction have been presented. It is of significance to the studies presented here that both the Subunit Dissociation Model[1] and the Disaggregation-Coupling Model[37] propose that the exchange of GTP for GDP is an essential and key event in the G-protein-coupled signal transduction pathway. The results described here may provide a new way to explore whether membrane lipids such as PA and LPA are involved in functional regulation of G-protein-coupled signal transduction by influencing GTP binding activity of G protein.

Both PA and LPA are believed to be bioactive lipid messengers. Preininger *et al.*[38] recently reported that βγ-subunits modulated phospholipase D directly. It is also worth noting that PA regulation of phospholipase C-β was determined structurally.[39] In addition, the GAP activity of RGS4, a regulator of G-protein signaling (RGS) proteins is inhibited by PA.[19] These findings

Table V

Differences between the LPA/PA/PS–Goα Complexes

Ligand	Glycerin backbone	Goα RMSD	Local distortion	Number of H Bond	ElecE (%)	VDWE (%)	InterE/MW
LPA	Extended	0.3	Small	4	72	28	0.43
PA	Folding	0.81	Medium	3	64	36	0.32
PS	Folding	0.75	Large	1	47	53	0.25

Goα RMSD, the difference in Goα backbone RMSD between before and after docking; elecE and VDWE, the percentages of electrostatic and VDW energy making up the total energy; InterE/MW, the total intermolecular energy divided by the molecular weight of the ligand. This scalar quantity is a token of the stability of the binding.

along with those in this current work imply that PA may play an important role in the G-protein-coupled signal transduction pathway.

CONCLUSION

The experimental results of the specific inhibition by PA on the GTP binding activity of Goα provided strong and direct biochemical evidences for their interaction, and the results of homology modeling and molecular docking proposed a model for the structural basis of this interaction. The experimental and modeling results matched well. The lipid–protein model suggested that PA may occupy the channel for exchanging guanine nucleotides, which leads to the inhibition. Our work also shed light on how membrane lipids may modulate the functions of Gα in G-protein-coupled signal transmembrane transduction pathway. These results could potentially lead the way to new drug targets for genetic diseases caused by genetic G-protein abnormalities.

ACKNOWLEDGMENTS

The authors are highly grateful to Dr. Geir Skogerb for his careful language corrections. This work is supported by grants from the National Basic Research Program of China (Grants 2004CB720000 and 2006CB911001).

REFERENCES

1. Gilman AG. G proteins: transducers of receptor-generated signals. Annu Rev Biochem 1987;56:615–649.
2. Neer EJ. Heterotrimeric G proteins: organizers of transmembrane signals. Cell 1995;80:249–257.
3. Offermanns S. G-proteins as transducers in transmembrane signalling. Prog Biophys Mol Biol 2003;83:101–130.
4. Sternweis PC, Robishaw JD. Isolation of two proteins with high affinity for guanine nucleotides from membranes of bovine brain. J Biol Chem 1984;259:13806–13813.
5. Jiang M, Gold MS, Boulay G, Spicher K, Peyton M, Brabet P, Srinivasan Y, Rudolph U, Ellison G, Birnbaumer L. Multiple neurological abnormalities in mice deficient in the G protein Go. Proc Natl Acad Sci 1998;95:3269–3274.
6. Wettschureck N, Offermanns S. Mammalian G proteins and their cell type specific functions. Physiol Rev 2005;85:1159–1204.
7. Jiang M, Spicher K, Boulay G, Wang Y, Birnbaumer L. Most central nervous system D2 dopamine receptors are coupled to their effectors by Go. Proc Natl Acad Sci 2001;98:3577–3582.
8. Ram PT, Horvath CM, Iyengar R. Stat3-mediated transformation of NIH-3T3 cells by the constitutively active Q205L Galphao protein. Science 2000;287:142–144.
9. Strittmatter SM, Fishman MC, Zhu XP. Activated mutants of the alpha subunit of G(o) promote an increased number of neurites per cell. J Neurosci 1994;14:2327–2338.
10. Jordan JD, He JC, Eungdamrong NJ, Gomes I, Ali W, Nguyen T, Bivona TG, Philips MR, Devi LA, Iyengar R. Cannabinoid receptor-induced neurite outgrowth is mediated by Rap1 activation through G(α)o/i-triggered proteasomal degradation of Rap1GAPII. J Biol Chem 2005;280:11413–11421.
11. Topham MK. Signaling roles of diacylglycerol kinases. J Cell Biochem 2006;97:474–484.
12. Jenkins GM, Frohman MA. Phospholipase D: a lipid centric review. Cell Mol Life Sci 2005;62:2305–2316.
13. English D, Cui Y, Siddiqui RA. Messenger functions of phosphatidic acid. Chem Phys Lipids 1996;80:117–132.
14. Rizzo M, Romero G. Pharmacological importance of phospholipase D and phosphatidic acid in the regulation of the mitogen-activated protein kinase cascade. Pharmacol Ther 2002;94:35–50.
15. Andresen BT, Rizzo MA, Shome K, Romero G. The role of phosphatidic acid in the regulation of the Ras/MEK/Erk signaling cascade. FEBS Lett 2002;53:65–68.
16. Fang Y, Vilella-Bach M, Bachmann R, Flanigan A, Chen J. Phosphatidic acid-mediated mitogenic activation of mTOR signaling. Science 2001;294:1942–1945.
17. Ghosh S, Strum JC, Sciorra VA, Daniel L, Bell RM. Raf-1 kinase possesses distinct binding domains for phosphatidylserine and phosphatidic acid. Phosphatidic acid regulates the translocation of Raf-1 in 12-*O*-tetradecanoylphorbol-13-acetate-stimulated Madin-Darby canine kidney cells. J Biol Chem 1996;271:8472–8480.
18. Frank C, Keilhack H, Opitz F, Zschornig O, Bohmer FD. Binding of phosphatidic acid to the protein–tyrosine phosphatase SHP-1 as a basis for activity modulation. Biochemistry 1999;38:11993–12002.
19. Ouyang YS, Tu Y, Barker SA, Yang F. Regulators of G-protein signaling (RGS) 4, insertion into model membranes and inhibition of activity by phosphatidic acid. J Biol Chem 2003;278:11115–11122.
20. Cao Y, Huang YG. Palmitoylation regulates GDP/GTP exchange of G protein by affecting the GTP-binding activity of Goα. Int J Biochem Cell Biol 2004;37:637–644.
21. Zhang L, Yang S, Huang Y. Evidence for disaggregation of oligomeric G(o) alpha induced by guanosine-5′-3-*O*-(thio)triphosphate activation. Biochemistry 2003;68:121–128. Moscow.
22. Northup JK, Smigel MD, Sternweis P, Gilman AG. The subunits of the stimulatory regulatory component of adenylate cyclase. Resolution of the activated 45,000-dalton (α) subunit. J Biol Chem 1983;258:11369–11376.
23. Sanchez-Bautista S, Marin-Vicente C, Gomez-Fernandez JC, Corbalan-Garcia S. The C2 domain of PKCα is a Ca^{2+}-dependent PtdIns(4,5)P2 sensing domain: a new insight into an old pathway. J Mol Biol 2006;362:901–914.
24. Corbalan-Garcia S, Sanchez-Carrillo S, Garcia-Garcia J, Gomez-Fernandez JC. Characterization of the membrane binding mode of the C2 domain of PKC epsilon. Biochemistry 2003;42:11661–11668.
25. Lakowicz J. Principles of fluorescence spectroscopy. New York: Plenum; 1983.
26. Graber R, Kasper P, Malashkevich VN, Sandmeier E, Berger P, Gehring H, Jansonius JN, Christen P. Changing the reaction specificity of a pyridoxal-5′-phosphate-dependent enzyme. Eur J Biochem 1995;232:686–690.
27. Posner BA, Mixon MB, Wall MA, Sprang SR, Gilman AG. The A326S mutant of Giα1 as an approximation of the receptor-bound state. J Biol Chem 1998;273:21752–21758.
28. Orry AJ, Wallace BA. Modeling and docking the endothelin G-protein-coupled receptor. Biophys J 2000;79:3083–3094.
29. Böhm HJ. The development of a simple empirical scoring function to estimate the binding constant for a protein–ligand complex of known three-dimensional structure. J Comp Aided Mol Des 1994;8:243–256.
30. Böhm HJ. Prediction of binding constants of protein ligands: a fast method for the prioritization of hits obtained from the de novo design or 3D database search programs. J Comp Aided Mol Des 1998;12:309–323.
31. Morris GM, Goodsell DS, Halliday RS, Huey R, Hart WE, Belew RK, Olson AJ. Automated docking using Lamarckian genetic algorithm and an empirical binding free energy function. J Comp Chem 1998;19:1639–1662.
32. Mancinelli F, Caraglia M, Budillon A, Abbruzzese A, Bismuto E. Molecular dynamics simulation and automated docking of the pro-apoptotic Bax protein and its complex with a peptide designed

from the Bax-binding domain of anti-apoptotic Ku70. J Cell Biochem 2006;99:305–318.
33. Lüthy R, Bowie JU, Eisenberg D. Assessment of protein models with three-dimensional profiles. Nature 1992;356:83–85.
34. InsightII User Guide. San Diego, CA: Accelrys; 1999.
35. Zhu LL, Hou TJ, Chen LR, Xu YJ. Molecular docking studies of the 4-anilinoquinazoline inhibitors with EGFR. Acta Chim Sin 2002;60:43–48.
36. Raw AS, Coleman DE, Gilman AG, Sprang SR. Structural and biochemical characterization of the GTPγS- GDPPi-, and GDP-bound forms of a GTPase-deficient Gly42 → Val mutant of Giα1 Biochemistry 1997;36:15660–15669.
37. Rodbell M. The complex regulation of receptor-coupled G-proteins. Adv Enzyme Regul 1997;37:427–435.
38. Preininger AM, Henage LG, Oldham WM, Yoon EJ, Hamm HE, Brown HA. Direct modulation of phospholipase D activity by Gβγ. Mol Pharmacol 2006;70:311–318.
39. Ross EM, Mateu D, Gomes AV, Arana C, Tran T, Litosch I. Structural determinants for phosphatidic acid regulation of phospholipase C-β1. J Biol Chem 2006;281:33087–33094.